

## OBSERVATIONS OF EUV WAVES IN <sup>3</sup>HE-RICH SOLAR ENERGETIC PARTICLE EVENTS

R. BUČÍK AND D. E. INNES AND L. GUO

Max-Planck-Institut für Sonnensystemforschung, D-37077 Göttingen, Germany and  
Max Planck/Princeton Center for Plasma Physics, Princeton, NJ 08540, USA

G. M. MASON

Applied Physics Laboratory, Johns Hopkins University, Laurel, MD 20723, USA

AND

M. E. WIEDENBECK

Jet Propulsion Laboratory, California Institute of Technology, Pasadena, CA 91109, USA

*Draft version September 6, 2015*

### ABSTRACT

Small <sup>3</sup>He-rich solar energetic particle (SEP) events with their anomalous abundances, markedly different from solar system, provide evidence for a unique acceleration mechanism that operates routinely near solar active regions. Although the events are sometimes accompanied by coronal mass ejections (CMEs) it is believed that mass and isotopic fractionation is produced directly in the flare sites on the Sun. We report on a large-scale extreme ultraviolet (EUV) coronal wave observed in association with <sup>3</sup>He-rich SEP events. In the two examples discussed, the observed waves were triggered by minor flares and appeared concurrently with EUV jets and type III radio bursts but without CMEs. The energy spectra from one event are consistent with so-called class-1 (characterized by power laws) while the other with class-2 (characterized by rounded <sup>3</sup>He and Fe spectra) <sup>3</sup>He-rich SEP events, suggesting different acceleration mechanisms in the two. The observation of EUV waves suggests that large-scale disturbances, in addition to more commonly associated jets, may be responsible for the production of <sup>3</sup>He-rich SEP events.

*Subject headings:* acceleration of particles — Sun: flares — Sun: particle emission — waves

### 1. INTRODUCTION

Discovered more than 40 years ago, <sup>3</sup>He-rich solar energetic particles (SEPs) are still poorly understood. The enormous abundance enhancement (up to factors of  $>10^4$ ) of the rare <sup>3</sup>He isotope is the most striking feature of these events, though large enhancements in heavy (Ne-Fe) and ultra-heavy nuclei are also observed (see Kocharov & Kocharov 1984; Mason 2007, for a review). Type III radio bursts with their parent low-energy electrons are firmly associated with <sup>3</sup>He-rich SEP events (Reames et al. 1985; Nitta et al. 2006). Solar sources of <sup>3</sup>He-rich SEPs are often accompanied by jet-like emissions in extreme ultraviolet (EUV) or X-ray images and sometimes in white-light reaching out to distances  $>2$  solar radii ( $R_{\odot}$ ) (Wang et al. 2006; Nitta et al. 2006, 2008). Somewhat surprisingly an association with fast and narrow coronal mass ejections (CMEs) has been reported in some <sup>3</sup>He-rich SEP events (Kahler et al. 2001; Nitta et al. 2006). CMEs with their driven shocks have been considered as a particle source for large gradual events while <sup>3</sup>He-rich SEPs are believed to be produced directly in flare sites presumably through gyroresonant wave-particle interactions (see review by Reames 2013). The CMEs associated with <sup>3</sup>He-rich SEP events may be considered to be high-altitude counterparts of reconnection X-ray jets discovered by Shibata et al. (1992).

What other signatures of solar activity can be associated with <sup>3</sup>He-rich SEPs? Recently Nitta et al. (2015)

describe the properties of a large sample (29) of <sup>3</sup>He-rich events with SDO observations of their solar source regions. About a half of the events were associated with jets and another half with wider eruptions. Four were associated with large scale disturbances (EUV waves) and slow ( $<350 \text{ km s}^{-1}$ ) CMEs. Coronal EUV waves in large gradual SEP events have been observed for almost two decades (Torsti et al. 1999). Some authors have recently attempted to explain SEP events observed at widely separate longitudes in terms of EUV waves (e.g., Rouillard et al. 2012; Park et al. 2013; Lario et al. 2014). At the outset of the eruption they appear to trace the progress of the shock responsible for particle acceleration. However, the association of EUV waves with <sup>3</sup>He-rich SEP events has seldom been discussed (Wiedenbeck et al. 2013; Nitta et al. 2015).

In this paper, we report on two <sup>3</sup>He-rich SEP events clearly associated with coronal EUV waves. The observations were made during a period of low solar activity in early 2010. We examine the relationship of the EUV waves to the accompanying energetic particles, including a detailed analysis of the wave fronts. It appears that the wave properties may be correlated with the observed ion spectra. These observations of SEP events and EUV waves are presented in section 2, and we discuss their implications in section 3.

### 2. OBSERVATIONS

The two <sup>3</sup>He-rich SEP events reported in this paper were identified using observations from the time-of-flight mass spectrometers Ultra Low Energy Isotope Spectrom-

eter (ULEIS; Mason et al. 1998) on the *Advanced Composition Explorer* (*ACE*) and the Suprathermal Ion Telescope (SIT; Mason et al. 2008) on the *Solar Terrestrial Relations Observatory AHEAD* spacecraft (*STEREO-A*). The responsible solar sources were examined in full-Sun images from the EUV imager (EUVI; Howard et al. 2008) on *STEREO*. *ACE* is in an orbit around the L1 point; *STEREO-A* is in a heliocentric orbit at  $\sim 1$  AU near the ecliptic plane moving faster than Earth at a rate of  $\sim 22^\circ$  per year.

### 2.1. $^3\text{He}$ -Rich SEP Events

Figure 1 shows two  $^3\text{He}$ -rich SEP events, one observed by *ACE* on 2010 January 26 (left panels) and another by *STEREO-A* on 2010 February 2 (right). These are among the first  $^3\text{He}$ -rich SEP events detected after the unusually long solar minimum between solar cycles 23 and 24 (the February 2 event is also identified in Wiedenbeck et al. (2013)). Both events were accompanied by energetic electron enhancements observed by EPAM/*ACE* (Gold et al. 1998) or SEPT/*STEREO-A* (Müller-Mellin et al. 2008) as shown in Figure 1a. The approximate onset of EPAM electron event on January 26 is at 17:25 UT (45 keV). The onset of SEPT electron event on February 2 is quite uncertain; the main increase starts around 12:00 UT (50 keV), but it was preceded by another minor event. Figure 1b shows individual ions in the helium mass range at 0.4-10 MeV nucleon $^{-1}$  for ULEIS/*ACE* and at 0.25-0.90 MeV nucleon $^{-1}$  for SIT/*STEREO-A*. The  $^3\text{He}$  track is clearly separated in ULEIS data. An examination of SIT mass histograms in the February 2 event confirms a clear  $^3\text{He}$  peak within the helium range (see Figure 2b). The January 26 event has a clear dispersive onset, where higher energy ions arrived earlier than lower energy ones as shown by the triangular pattern in the inverted ion-speed time spectrogram in Figure 1c. The February 2 event could also have been dispersive, but it is possible that a magnetic-cloud like structure may have reduced the intensity of energetic ions (e.g., Cane & Lario 2006). The interplanetary magnetic field (IMF) data from the MAG/*ACE* instrument (Acuña et al. 2008) shows a smooth rotation of the magnetic field vector during 14-20 UT (see Figure 1c). The 320-450 keV nucleon $^{-1}$   $^3\text{He}/^4\text{He}$  ratio is 0.13 for January 26 and 0.41 for February 2 event. The Fe/O ratio is  $\sim 0.6$  in both events; somewhat smaller than the average value in  $^3\text{He}$ -rich flares (cf.  $\sim 0.95$  at 385 keV nucleon $^{-1}$  in Mason et al. 2004).

The January 26 event was associated with a B3.2 *GOES* X-ray flare in active region (AR) 1042 (N20°W75°) with a start time at 17:01 UT (Solar Events List<sup>1</sup>). Close to the time of the flare onset, a strong type III radio burst was observed by WAVES/*WIND* (Bougeret et al. 1995) (see Figure 1d). The estimated ion solar release time from extrapolation of ULEIS spectrogram data to the zero propagation time is around the type III burst onset, though uncertainty arising from this technique has been reported to be  $\pm 45$  minutes (Mason et al. 2000). Less clear is the ion release time in the February 2 event. The event (from different AR; see Section 2.3) may be related to the preceding main electron increase and associated type III burst at 11:42 UT mea-

sured by WAVES/*STEREO-A* (Bougeret et al. 2008); other type III bursts preceding the event occurred at 10:24 and 07:04 UT (see Figure 1d). The burst at 07:04 UT is also significant, extending to both high and low frequencies, and may be associated with an observed minor electron intensity increase. Hereafter, we focus on the type III burst at 11:42 UT because it was associated with the main electron event. The Solar Radio Bursts report<sup>2</sup> includes type III at 17:03 on January 26 in frequency range 25-144 MHz (Sagamore Hill) and type III at 07:04 on February 2 in 20-130 MHz (Culgoora). The type III at 11:42 UT on February 2 extended into the range 20-70 MHz<sup>3</sup> (Nançay Decameter array). No metric type II radio bursts were observed in these two events.

Figure 2a shows event averaged fluence spectra for January 26 and Figure 2b shows the spectra for the February 2  $^3\text{He}$ -rich SEP event. The January 26 spectra for  $^3\text{He}$ ,  $^4\text{He}$ , O, and Fe have similar power laws. They are reminiscent of class-1 event spectra where major species exhibit similar power laws or broken power laws with  $^3\text{He}$  often showing stronger hardening below  $\sim 1$  MeV nucleon $^{-1}$  (Mason et al. 2000, 2002). In the February 2 event,  $^4\text{He}$  and O have similar power laws but the  $^3\text{He}$  and Fe spectra are distinctly flatter, leading to a larger variation of  $^3\text{He}/^4\text{He}$  and Fe/O with energy than in the January 26 event. The February 2 event spectra are similar to class-2 event spectra, characterized by curved  $^3\text{He}$  and Fe spectra towards low energies with  $^3\text{He}$  rollovers in the range  $\sim 100$ -600 keV nucleon $^{-1}$  and Fe rollovers below  $\sim 100$  keV nucleon $^{-1}$  (Mason et al. 2000). Certainly, the spectral shapes in these two events are not very representative of class-1 or class-2 events. There are fluctuations at several spectral points making it somewhat difficult to categorize the January 26 event solely by its  $^3\text{He}$  shape. Note, the median value of  $^3\text{He}/^4\text{He}$  ratio of class-1 events ( $\sim 0.12$  at 385 keV nucleon $^{-1}$  in Mason et al. 2002) is strikingly similar to  $^3\text{He}/^4\text{He}$  ratio in the January 26 event.

### 2.2. EUV Wave - January 26 Event

During the investigated events the *ACE* and *STEREO-A* were angularly separated by  $65^\circ$  allowing the nearest limb regions from *ACE* to be observed in a more direct view by *STEREO-A*. We emphasize that such a constellation enables a completely new insight on  $^3\text{He}$ -rich sources, not available in earlier investigations. Figure 3 (left) shows the EUV 195 Å image of AR 1042 near the central meridian in the *STEREO-A* view. Running difference images in Figure 3 (right) show jet-like emissions at 17:00-17:05 UT in the eastern foot-point of a series of small magnetic loops. The observed temporal coincidence between the EUV jet in AR 1042 and the type III burst indicates that the AR contains open field allowing particles to escape.

A large-scale wave was observed emanating from AR 1042, the  $^3\text{He}$ -rich SEP source, as demonstrated in running difference images in Figure 3. The wave was clearly seen even in direct EUV images (see animation of Figure 3 (left)). The launch time of the wave temporally coincides with the EUV jet. A bright wave front was

<sup>1</sup> [www.swpc.noaa.gov](http://www.swpc.noaa.gov)

<sup>2</sup> [ftp.ngdc.noaa.gov](http://ftp.ngdc.noaa.gov)

<sup>3</sup> [secchirh.obspm.fr](http://secchirh.obspm.fr)

clearly seen at 17:05 UT ( $\sim 4$  minutes after the X-ray flare and 2 minutes after the type III) but a weaker arc-shaped dimming, probably associated with the wave, was already seen at the type III burst onset. The wave front propagated southward towards the equator and nominal spacecraft foot-point based on the Parker spiral model. The nominal foot-point location was not reached before 17:15 UT, but the electron, and likely also the ion, release was associated with the jet, type III burst and the wave-launch that occurred earlier. Thus the wave could already intersect the open field lines connecting to the spacecraft at the time when it started.

The nose of the wave front traveled  $15^\circ$  in latitude between 17:03 and 17:13 UT, which corresponds roughly to  $300 \text{ km s}^{-1}$ . This is within the range ( $200\text{-}400 \text{ km s}^{-1}$ ) of typical EUV wave speeds (Thompson & Myers 2009) and is comparable with quiet-Sun fast magnetosonic speeds. Previous observations have shown that EUV waves can be faster in the early stage and may even be shocks (e.g., Warmuth & Mann 2011). Indeed, newer high-cadence observations, capable of capturing the initial phases of the wave evolution, indicate much higher speeds ( $\sim 600 \text{ km s}^{-1}$ ; Nitta et al. 2013) implying that these waves may steepen to shocks quite frequently. EUV wave shocks directly observed as dome-like enhancements propagating ahead of a CME have been reported in some recent investigations (Veronig et al. 2010; Kozarev et al. 2011; Ma et al. 2011).

The EUV image of the Sun's disk in Figure 3 reveals quite uniform coronal structure with the only other AR located far away, near the south-east solar limb and a coronal hole at the south-pole. This likely enabled undisturbed wave propagation and therefore its easier observation. Note that ARs/coronal holes in the paths of the waves usually cause them to fade/reflect (e.g., Thompson et al. 1999). The fact that AR 1042 is quite isolated with no simultaneous activity observed in other regions also allowed a more straightforward identification of the  $^3\text{He}$ -rich SEP source. Note that many  $^3\text{He}$ -rich SEP events have been left without identified solar sources, for example, 40% out of 117 events by Nitta et al. (2006).

The driver of EUV waves has often been associated with CMEs but in this event there was no CME. Any CME associated with January 26 event would be best visible in a coronagraph from the Earth view because of the source location near the western limb. The SOHO LASCO C2 observations, covering the range  $1.5\text{-}6 R_\odot$ , show a narrow stream at 17:54, 18:06 and 18:30 UT at near-equatorial region on the west. In SOHO LASCO CME catalog<sup>4</sup> this brief eruption was classified as a very poor event. No eruption was seen from  $1.4$  to  $4 R_\odot$  in STEREO-A COR-1 5-minute running difference images<sup>5</sup>. Also the STEREO COR1 preliminary list<sup>6</sup> indicates no associated CME.

### 2.3. EUV Wave - February 2 Event

Figure 4 (left) shows the STEREO-A EUV 195 Å image of the solar source AR for the February 2  $^3\text{He}$ -rich SEP event, located at  $\text{N}20^\circ\text{W}65^\circ$  from STEREO-A, which was  $65^\circ$  west of the Sun-Earth line. Running dif-

ference images in Figure 4 (right) show a jet at 11:45 UT, temporally coincident with a type III burst shown in Figure 1d. Similar to the previous event, the jet was emitted from the Sun's surface at the eastern foot-point of a series of small-scale loops. The AR emerged on 2010 January 30 when it was at the west limb as seen from the Earth. The running difference images in Figure 4 show a bright wave front emitted from the AR around the time of the jet and propagating in the south-east direction. The wave reached STEREO-A nominal foot-point around 12 UT, but the electron (and likely the ion also) release occurred earlier at 11:45 UT in association with the jet and the type III radio burst. The wave front in the February 2 event appears to be more diffuse (cf. wave fronts 12-13 min after type III burst onsets in both events at 17:15 and 11:55 UT) and less bright than in the January 26 event (cf. wave fronts 7-8 min after type III burst onsets in both events at 17:10 and 11:50 UT). The projection effects in the February 2 event probably play a minor role as the wave propagates toward the central meridian where these effects are less dominant. Because of the diffuse fronts in the February 2 event it is more difficult to measure the wave speed. A rough estimate is  $\gtrsim 200 \text{ km s}^{-1}$  between 11:45 and 12:00 UT where the wave front traveled  $15^\circ$  in the latitude. In direct EUV images the wave was not so clearly seen (see animation of Figure 4 (left)) as in the previous event. Note that in the February 2 event, STEREO-A provides only 5 minute cadence images while in January 26 event the cadence is 2.5 minutes. Thus, insufficient temporal resolution may be one reason why these waves were not noticed in earlier  $^3\text{He}$ -rich SEPs investigations. The above mentioned projection effects due to western location of  $^3\text{He}$ -rich sources may also add to the difficulty in an identification of the associated waves. The less intense type III burst at 10:25 UT (see Figure 1d) was also associated with a jet and a coronal wave but these were less significant than in the 11:42 UT type III burst. The type III at 07:04 UT also coincided with EUV brightening in the same AR but no wave was observed. The STEREO-A COR1 running difference images showed from 12:15 UT onward a small bright feature moving outward towards the west. This weak outflow was not marked in the COR-1 Preliminary CME List.

### 2.4. EUV Wave Profiles

In addition to a visual inspection as given in the previous sections, we also provide a quantitative analysis of the wave fronts. Figure 5 shows the evolution of the wave front profiles within 12 and 13 minutes after the associated type III radio bursts in the January 26 and February 2 events, respectively. A similar approach where the intensity ratios are derived along the propagating fronts is presented in earlier studies (e.g., Veronig et al. 2010). The figure reveals that the amplitudes of the intensity ratio and their temporal fluctuations are larger for the January 26 wave. The temporal behavior of the trailing front edges suggests that the January 26 wave was likely accelerating while the February 2 wave was moving with more uniform speed. These profiles also indicate lower speed for the February 2 wave.

## 3. DISCUSSION AND SUMMARY

<sup>4</sup> [cdaw.gsfc.nasa.gov/CME\\_list](http://cdaw.gsfc.nasa.gov/CME_list)

<sup>5</sup> [cdaw.gsfc.nasa.gov/STEREO/daily\\_movies](http://cdaw.gsfc.nasa.gov/STEREO/daily_movies)

<sup>6</sup> [cor1.gsfc.nasa.gov/catalog](http://cor1.gsfc.nasa.gov/catalog)

This paper examines a new solar phenomenon observed in association with  $^3\text{He}$ -rich SEPs. We present two events, where in addition to EUV jets,  $^3\text{He}$ -rich source ARs launched simultaneously a coronal EUV wave. The waves were initiated by minor flares and not linked to CMEs. The EUV waves have been considered to be closely related with CMEs (Biesecker et al. 2002), though recent investigations (Nitta et al. 2013) indicate that the association is not so strong.

The EUV waves may be a more common feature in  $^3\text{He}$ -rich SEP events than previously thought. Wiedenbeck et al. (2013) have noticed large-scale disturbances in the source region of the STEREO-B 2010 February 7 and ACE February 8  $^3\text{He}$ -rich SEP events. They have suggested that EUV waves could be responsible for a sympathetic flaring in a region far from the nominal connection and thus contributing to a wide particle longitude distribution. In a parallel study, Nitta et al. (2015) have reported large scale propagating fronts in a few  $^3\text{He}$ -rich SEP events on ACE by examining also active periods of a current solar cycle. Note that some other  $^3\text{He}$ -rich SEP events like 2008 November 4 on ACE (Mason et al. 2009) or 2011 July 1 on STEREO-B (Bučík et al. 2014) are also associated with EUV waves (not mentioned in original studies). Their sources are well visible near the central meridian similarly to the 2010 January 26 event.

Coronal jets, a signature of magnetic reconnection between magnetic loops and overlying open field (Shibata et al. 1992), create turbulence for  $^3\text{He}$ -rich SEP acceleration (e.g., Miller 1998; Petrosian 2012). Nearly all models of  $^3\text{He}$ -rich SEPs require some kind of two-stage processes. For example electrons, accelerated by cascading turbulence, excite plasma waves (Miller 1998) capable of gyroresonant interaction with ambient  $^3\text{He}$  (Temerin & Roth 1992). An alternative to turbulence is the reconnection-exhaust ion heating followed by an interaction with multiple magnetic islands (e.g., Drake & Swisdak 2012). The two spectral classes of  $^3\text{He}$ -rich SEPs is a relatively new feature, and have not yet been adequately explained. It has been suggested that class-2 events represent the basic mechanism of  $^3\text{He}$  enrichment and that class-1 events need a further stage of acceleration (e.g. by a shock wave) that may modify the spectra (Mason et al. 2002). A recent study by Nitta et al. (2015) indicated a slight tendency for events with jets at their source to have class-2 spectra (9 of 13), and those with EUV waves at their source to have class-1 spectra (3 of 4).

The observation of EUV waves, which may be shocks in their early phases, calls into question the details of  $^3\text{He}$ -rich SEP acceleration. The shape of the energy spectra observed in the first event, when the wave was bright, is similar to class-1 events. In this example the wave might have been capable of modifying the original curved spectra created by turbulence or by the pick-up mechanism in the reconnection exhausts. Biesecker et al. (2002) noted that EUV waves with bright, sharp fronts may indicate shocks. In the second event, where the wave front was less bright and perhaps slower, the spectral forms were consistent with the class-2 events, suggesting that the influence of the wave was minor. The energy spectra of  $^3\text{He}$  and  $^4\text{He}$  in the February 2 event are quite similar to spectra in the class-2 event on 1999 September 30 (Mason

et al. 2000), which were excellently fitted by stochastic acceleration (Figure 9 in Liu et al. 2006). We need to examine more events in order to evaluate the relevance of EUV waves on the two class spectra of  $^3\text{He}$ -rich SEPs. The two examples presented here also raise the question whether EUV waves themselves (even not steepened into the shocks) may generate or enhance turbulence required for  $^3\text{He}$ -rich SEP acceleration models.

We are grateful to the referee for valuable comments that helped to improve the manuscript. This work was supported by the Max-Planck-Gesellschaft zur Förderung der Wissenschaften. The STEREO SIT is supported by the Bundesministerium für Wirtschaft through the Deutsches Zentrum für Luft- und Raumfahrt (DLR) under grant 50 OC 1301. ACE/ULEIS and STEREO/SIT are supported at APL by NASA grant NNX13AR20G/115828 and NASA through subcontract SA4889-26309 from the University of California Berkeley. The work at JPL and Caltech was supported through subcontract SA2715-26309 from UC Berkeley under NASA contract NAS5-03131T, and by NASA grants NNX11A075G and NNX13AH66G.

#### REFERENCES

- Acuña, M. H., Curtis, D., Scheifele, J. L., et al. 2008, *Space Sci. Rev.*, 136, 203
- Biesecker, D. A., Myers, D. C., Thompson, B. J., Hammer, D. M., & Vourlidas, A. 2002, *ApJ*, 569, 1009
- Bougeret, J. L., Goetz, K., Kaiser, M. L., et al. 2008, *Space Sci. Rev.*, 136, 487
- Bougeret, J.-L., Kaiser, M. L., Kellogg, P. J., et al. 1995, *Space Sci. Rev.*, 71, 231
- Bučík, R., Innes, D. E., Mall, U., et al. 2014, *ApJ*, 786, 71
- Cane, H. V. & Lario, D. 2006, *Space Sci. Rev.*, 123, 45
- Drake, J. F. & Swisdak, M. 2012, *Space Sci. Rev.*, 172, 227
- Gold, R. E., Krimigis, S. M., Hawkins, S. E., et al. 1998, *Space Sci. Rev.*, 86, 541
- Howard, R. A., Moses, J. D., Vourlidas, A., et al. 2008, *Space Sci. Rev.*, 136, 67
- Kahler, S. W., Reames, D. V., & Sheeley Jr., N. R. 2001, *ApJ*, 562, 558
- Kocharov, L. G. & Kocharov, G. E. 1984, *Space Sci. Rev.*, 38, 99
- Kozarev, K. A., Korreck, K. E., Lobzin, V. V., Weber, M. A., & Schwadron, N. A. 2011, *ApJ*, 733, L25
- Lario, D., Raouafi, N. E., Kwon, R.-Y., et al. 2014, *ApJ*, 797, 8
- Liu, S., Petrosian, V. & Mason, G. M. 2006, *ApJ*, 636, 462
- Ma, S., Raymond, J. C., Golub, L., et al. 2011, *ApJ*, 738, 160
- Mason, G. M. 2007, *Space Sci. Rev.*, 130, 231
- Mason, G. M., Dwyer, J. R., & Mazur, J. E. 2000, *ApJ*, 545, L157
- Mason, G. M., Gold, R. E., Krimigis, S. M., et al. 1998, *Space Sci. Rev.*, 86, 409
- Mason, G. M., Korth, A., Walpole, P. H., et al. 2008, *Space Sci. Rev.*, 136, 257
- Mason, G. M., Mazur, J. E., Dwyer, J. R., et al. 2004, *ApJ*, 606, 555
- Mason, G. M., Nitta, N. V., Cohen, C. M. S., & Wiedenbeck, M. E. 2009, *ApJ*, 700, L56
- Mason, G. M., Wiedenbeck, M. E., Miller, J. A., et al. 2002, *ApJ*, 574, 1039
- Miller, J. A. 1998, *Space Sci. Rev.*, 86, 79
- Müller-Mellin, R., Böttcher, S., Falenski, J., et al. 2008, *Space Sci. Rev.*, 136, 363
- Nitta, N. V., Mason, G. M., Wang, L., Cohen, C. M. S., & Wiedenbeck, M. E. 2015, *ApJ*, 806, 235
- Nitta, N. V., Mason, G. M., Wiedenbeck, M. E., et al. 2008, *ApJ*, 675, L125
- Nitta, N. V., Reames, D. V., DeRosa M. L., et al. 2006, *ApJ*, 650, 438
- Nitta, N. V., Schrijver, C. J., Title, A. M., & Liu, W. 2013, *ApJ*, 776, 58
- Park, J., Innes, D. E., Bucik, R., & Moon, Y.-J. 2013, *ApJ*, 779, 184
- Petrosian, V. 2012, *Space Sci. Rev.*, 173, 535
- Reames, D. V. 2013, *Space Sci. Rev.*, 175, 53

- Reames, D. V., von Rosenvinge, T. T., & Lin, R. P. 1985, *ApJ*, 292, 716
- Rouillard, A. P., Sheeley, N. R., Tylka, A., et al. 2012, *ApJ*, 752, 44
- Shibata, K., Ishido, Y., Acton, L. W., et al. 1992, *PASJ*, 44, L173
- Temerin, M. & Roth, I. 1992, *ApJ*, 391, L105
- Thompson, B. J., Gurman, J. B., Neupert, W. M., et al. 1999, *ApJ*, 517, L151
- Thompson, B. J. & Myers, D. C. 2009, *ApJS*, 183, 225
- Torsti, J., Kocharov, L. G., Teittinen, M., & Thompson, B. J. 1999, *ApJ*, 510, 460
- Veronig, A. M., Muhr, N., Kienreich, I. W., Temmer, M., & Vršnak, B. 2010, *ApJ*, 716, L57
- Wang, Y.-M., Pick, M., & Mason, G. M. 2006, *ApJ*, 639, 495
- Warmuth, A. & Mann, G. 2011, *A&A*, 532, A151
- Wiedenbeck, M. E., Mason, G. M., Cohen, C. M. S., et al. 2013, *ApJ*, 762, 54

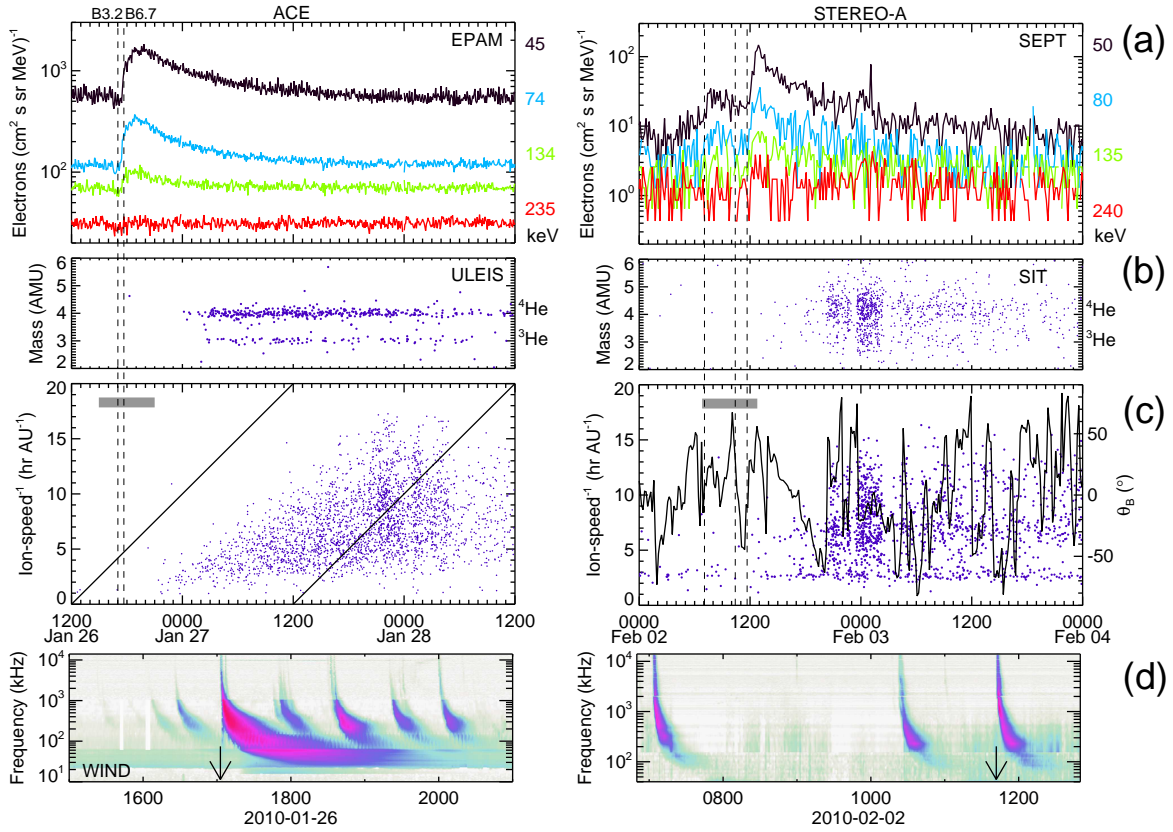


**Figure 1.** (a) 5 minute EPAM/ACE (left) and 10 minute SEPT/STEREO-A (right) electron intensities. (b) ULEIS/ACE 0.4-10 MeV nucleon $^{-1}$  (left) and SIT/STEREO-A 0.25-0.90 MeV nucleon $^{-1}$  (right) He mass spectrograms. (c) ULEIS (left) and SIT (right) spectrograms of 1/ion-speed versus arrival times of 10-70 amu ions. Sloped lines (left) indicate arrival times for particles traveling along a field line of 1.2 AU without scattering. Black curve (right) is the magnetic field zenith angle in Radial-Tangential-Normal (RTN) coordinates. The dashed vertical lines mark the start times of the GOES X-ray flares (left) and type III bursts (right). (d) radio spectrogram from WIND (left) and STEREO-A (right) WAVES instruments during 6 hr periods indicated by horizontal shaded bars in panels (c). The arrows mark type III bursts associated with the events.

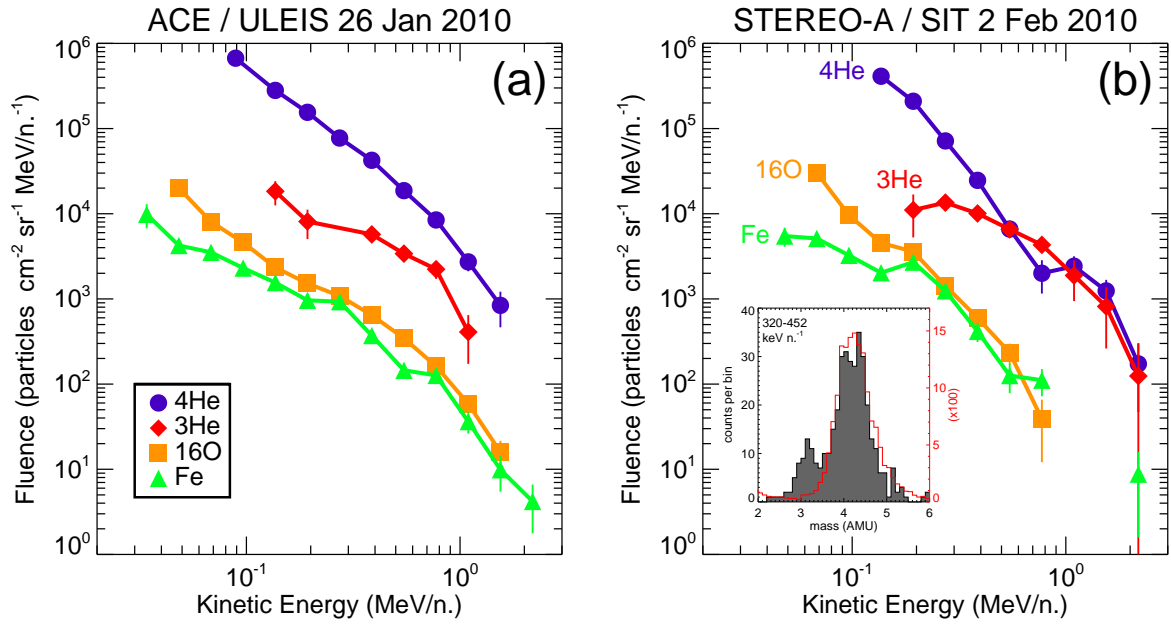


**Figure 2.** Energy spectra for January 26 (a) and February 2 (b)  $^3\text{He}$ -rich SEP events. Gray shaded histogram is for February 2 event. Red histogram is for corotating interaction region events (2010 May-June) to compare SIT observations with no  $^3\text{He}$  mass peak.

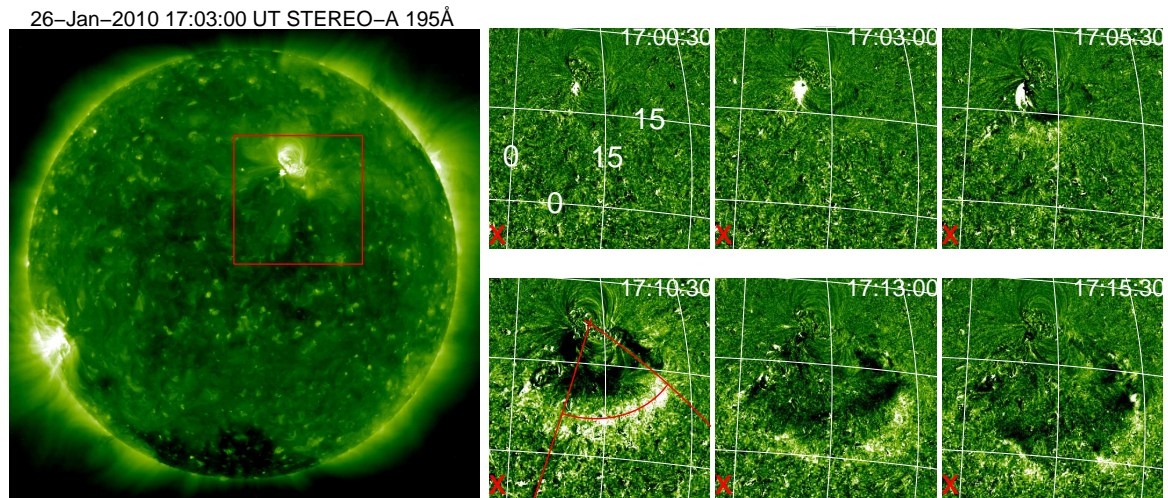


**Figure 3.** (Left) *STEREO-A* 195 Å EUV image of the solar disk on 2010 January 26 17:03 UT. (Right) six panels - 2.5 minute (except for 17:10:30, which is 5 min) running difference images of the area around AR 1042 marked by red square in the direct image. Red crosses indicate nominal foot-point of IMF line connecting to L1. Two red curves, passing through the AR (panel 17:10:30), indicate a 70° arc sector on the solar sphere where the EUV intensity profiles in Figure 5 were determined. The red curve along the wave front outlines an arc centered on the AR.  
(An animation of this figure is available.)



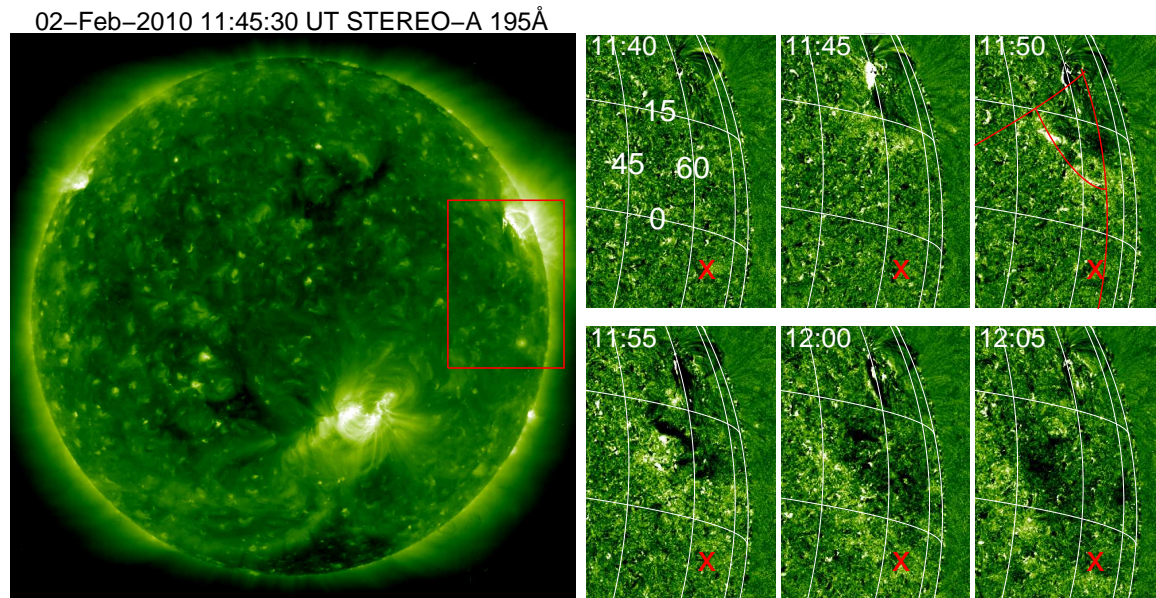


**Figure 4.** (Left) STEREO-A 195 Å EUV image of the solar disk on 2010 February 2 11:45 UT. (Right) six panels - 5 minute running difference images of the area marked by red square in the direct image. Red crosses indicate foot-point for STEREO-A. The red curves in the panel 11:50 have the same meaning as in Figure 3. (An animation of this figure is available.)

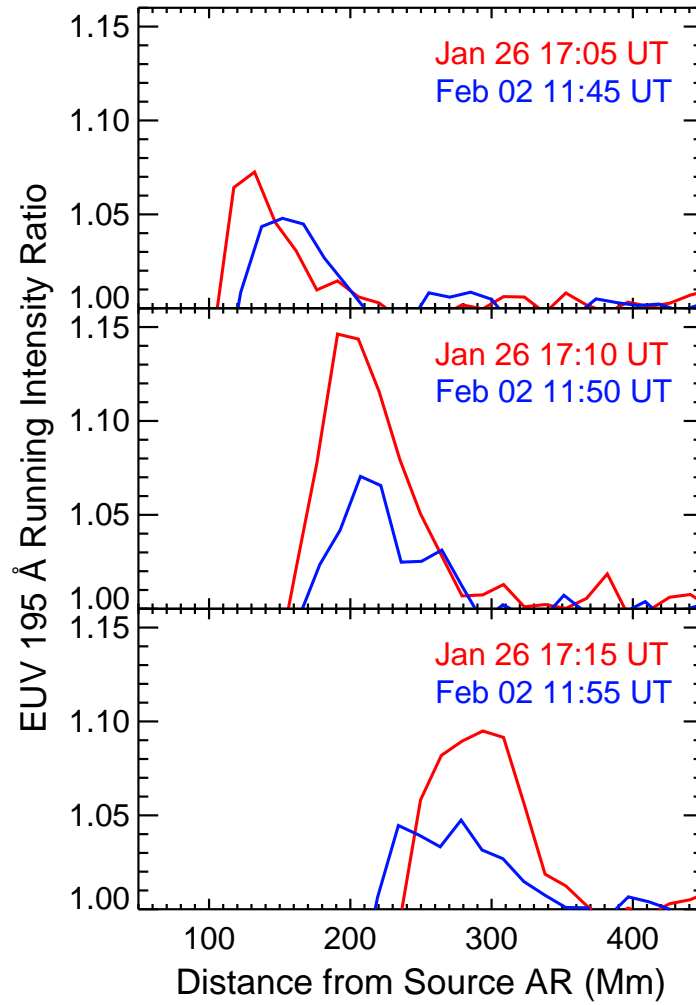


**Figure 5.** Average EUV intensity-ratio profiles for the January 26 (red curve) and February 2 (blue curve) wave fronts at three different times. The average ratios were determined in a  $70^\circ$  annular sectors with radial width 15 Mm and center in the source AR. The  $70^\circ$  arc sectors were placed on the brightest portion of the wave fronts (see Figures 3 and 4).